



Cite this: *Analyst*, 2025, **150**, 5457

## A sustainable and novel LC-TQ-MS/MS method for quantifying mutagenic Ketoconazole-NDSRIs aligned with green and white analytical chemistry principles

Srinivas Nakka, <sup>a</sup> Vishnu Murthy Marisetti <sup>b</sup> and Surendra Babu Manabolu Surya <sup>\*a</sup>

Fungal infections affect millions of people globally, ranging from minor skin conditions to life-threatening diseases. Ketoconazole (KCZ)MS, a potent synthetic imidazole, remains widely prescribed. This study reports the synthesis of *N*-nitrosoacetyl(piperazine) (*N*-NAP), a nitroso derivative of a KCZ-degradant, with the *N*-nitroso group confirmed by  $^1\text{H}$ - $^{15}\text{N}$  HMBC spectroscopy, and their genotoxic potential was evaluated using two (Q)SAR tools. The identified KCZ NDSRIs are categorized as class-3 as per QSAR, and the predictions showed as genotoxic positive (Cohort-of-concern). The acceptable intake (AI) levels of both nitrosamines were determined using the carcinogenic potency categorization approach (CPCA) and belonged to potency category-3. Following ICH Q14 recommendations, the LC-TQ-MS/MS method was optimized for the detection and quantification of KCZ-NDSRIs at trace amounts in KCZ pharmaceuticals. This study advances two Sustainable Development Goals (SDGs). It supports SDG 3 (good health and well-being, targets 3.8 & 3.d) by utilizing (Q)-SAR and CPCA analyses and contributes to SDG 9 (industry, innovation, and infrastructure, target 9.4) via a validated LC-TQ-MS/MS method for quantifying NDSRIs as per ICH Q2(R2). The chromatographic separation was optimized using a Waters X-bridge BEH C18 column (150 mm x 2.1 mm, 2.5  $\mu\text{m}$ ) with gradient elution. Mobile phases consisted of 0.1% formic acid in water and acetonitrile with a column oven temperature of 40 °C and a pump flow rate of 0.4 mL min $^{-1}$ . Aligned with ICH Q14, this approach defines the analytical target profile (ATP) and established conditions (ECs) and incorporates risk assessment and reporting categories. The robustness and validation of the current method were executed following the ICH Q2(R2) guidelines. The sustainability of the proposed method was demonstrated using cutting-edge tools, like AGREE, Modified GAPI, BAGI, RAPI CaFRI and RGB12, reinforcing its white and green and sustainable nature.

Received 2nd October 2025,  
Accepted 30th October 2025

DOI: 10.1039/d5an01052g  
[rsc.li/analyst](http://rsc.li/analyst)

### 1. Introduction

NDSRIs (nitrosamine drug substance-related impurities) are a subclass of nitrosamines that specifically arise during the synthesis, storage, or degradation of pharmaceutical drug substances or their intermediates. NDSRIs may also be formed during the manufacturing processes and storage of pharmaceutical drug products. Unlike general nitrosamine contaminants that might enter from external sources (such as solvents, reagents, or packaging), NDSRIs are intrinsically linked to the molecular structure or chemical reactivity of the active pharmaceutical ingredient (API) itself.<sup>1–4</sup> In contrast to simple nitrosamines with recurring structural patterns, NDSRIs show

considerable diversity and typically contain elements of the parent drug molecule.

Degradation mechanisms describe the chemical reactions that cause APIs to decompose over time or when exposed to certain environmental factors, resulting in the formation of impurities.<sup>5,6</sup> The pathways for NDSRI formation usually involve a direct reaction between a drug substance with a secondary amine moiety and nitrosating agents, such as nitrites or nitrates, under acidic conditions. Further, the possibilities extend to the generation of secondary amines formed due to DS degradation or process carryovers that can react with nitrosating agents.<sup>7</sup> Key degradation mechanisms leading to the formation of NDSRI precursors, such as secondary amines, include hydrolysis, oxidation, photolysis, thermal decomposition, and acid-/base-catalysed degradation. The formation of various NDSRIs as degradation impurities is summarized in Table 1.<sup>8–17</sup>

Fungal infections affect millions of patients worldwide and encompass a wide clinical spectrum, from superficial dermal

<sup>a</sup>Department of Chemistry, School of Science, GITAM Deemed to be University, Hyderabad-502329, India. E-mail: [smanabol@gitam.edu](mailto:smanabol@gitam.edu)

<sup>b</sup>ScieGen Pharmaceuticals Inc., Quality Assurance, 89 Arkay Drive, Hauppauge, New York, USA 11788



**Table 1** Various NDSRI formation from degradation pathways

API	Stress conditions/ process carryovers	Secondary amine precursor	Reaction with nitrosating agent	NDSRI formed	References
Valsartan	Hydrolysis/process impurities	Amine-containing intermediates		Valsartan-related NDSRIs (complex nitrosamines)	EMA and FDA reports on valsartan nitrosamine impurities <sup>8,9</sup>
Irbesartan	Hydrolysis/process impurities	Amine-containing intermediates		Irbesartan NDSRIs	Reported in recalls and impurity investigations <sup>10</sup>
Saxagliptin	Thermal/oxidative degradation	Secondary amine degradation products		Saxagliptin-specific nitrosamines	Analytical studies and stability reports <sup>11</sup>
Vildagliptin	Acid-/base-catalyzed degradation	Amine-containing impurities	Nitrates/nitrites	Vildagliptin NDSRIs	Found in stability studies <sup>12</sup>
Avanafil	Thermal degradation	Amino intermediates	Possible sources from water, nitrite salts, and excipients.	Avanafil-related nitrosamines	Degradation impurity reports <sup>13</sup>
Ranolazine	Oxidation/thermal degradation	Amino degradation products		Ranolazine-related NDSRIs	Stability studies showing nitrosamines <sup>14</sup>
Empagliflozin	Thermal/acid-catalyzed degradation	Amine degradation products		Empagliflozin-specific NDSRIs	Recent impurity screening <sup>15,16</sup>
Linagliptin	Thermal and photolytic degradation	Amine-containing degradation products		Linagliptin NDSRIs	Pharmaceutical degradation studies <sup>17</sup>

infections to invasive, life-threatening mycoses.<sup>18,19</sup> Ketoconazole (KCZ), a synthetic imidazole introduced in the late 20th century, has been extensively used owing to its anti-fungal efficacy. Its mechanism of action involves inhibition of fungal lanosterol 14 $\alpha$ -demethylase, a cytochrome P450-dependent enzyme that plays a central role in ergosterol synthesis, ultimately compromising the structural integrity of the fungal cell membrane.<sup>20,21</sup> Beyond its antifungal effects, it also possesses antiandrogenic properties, which have led to its off-label use under conditions such as Cushing's syndrome and androgenic alopecia.<sup>22</sup> Projections indicate a compound annual growth rate (CAGR) of approximately 3.1% for the global KCZ market over the period 2023–2030. This growth is primarily attributed to the rising demand for antifungal therapies and advancements in drug delivery technologies.<sup>23</sup>

A systematic review of KCZ degradation studies revealed consistent findings across analytical reports, indicating that both acidic and basic hydrolysis pathways lead to a common degradant *via* *N*-acetyl cleavage and the subsequent formation of a piperazine-based cyclic secondary amine<sup>24–27</sup>—a potential precursor for the formation of NDSRI under certain storage conditions. In recent years, the control of nitrosamine impurities in pharmaceuticals has become crucial and concerning because of the cohort of concern, which leads to cancer in humans upon longer exposure periods. Hence, the control of such toxic nitrosamine impurities at their lowest limits requires sophisticated, advanced analytical techniques and highly sensitive analytical methods. Our extensive literature search review reveals that there is currently no established analytical method that can detect KCZ-degradant NDSRIs at trace levels in KCZ formulations. To address this critical research gap, we leveraged LC-MS using an MRM approach, enhancing both sensitivity and specificity in detecting KCZ-

degradant NDSRIs. In this case study, we report the synthesis and structural characterization of select KCZ-degradant NDSRIs, along with the development and validation of a highly sensitive LC-TQ-MS/MS analytical method. This method was designed in accordance with the revised ICH guidelines for the identification and trace-level quantification of these impurities in KCZ formulations.

Green Analytical Chemistry (GAC) focuses on developing sustainable, energy-efficient analytical methods. As green technologies and regulations advance, GAC is set to guide future practices. Gałuszka *et al.* outlined twelve principles of GAC, adapted from green chemistry.<sup>28,29</sup> The environmental impact of the proposed method was evaluated using multiple greenness and sustainability assessment tools, including the AGREE, Modified Green Analytical Procedure Index (MoGAPI), Blue Applicability Grade Index (BAGI), Red Analytical Performance Index (RAPI), and Carbon Footprint Reduction Index (CaFRI). Additionally, the method's overall whiteness was assessed using the RGB12 model.

As a collective promise to humanity, the 2030 Agenda was adopted in 2015 by every UN member nation. It lays out 17 interconnected Sustainable Development Goals (SDGs) that serve as a global roadmap toward universal well-being, environmental stewardship, and human-centred innovation.<sup>30</sup> In alignment with the SDGs, this research contributes to two key areas. SDG 3 (Good Health and Well-Being) promotes medicine safety (Target 3.8) and risk management (Target 3.d) through the application of (Q)-SAR and CPCA analyses to evaluate NDSRI-related risks. In support of SDG 9 (Industry, Innovation, and Infrastructure), this study advances sustainable technology (Target 9.4) by developing a novel and eco-friendly LC-TQ-MS/MS method for the simultaneous quantification of KCZ-degradant NDSRIs (Fig. 1). This study not only



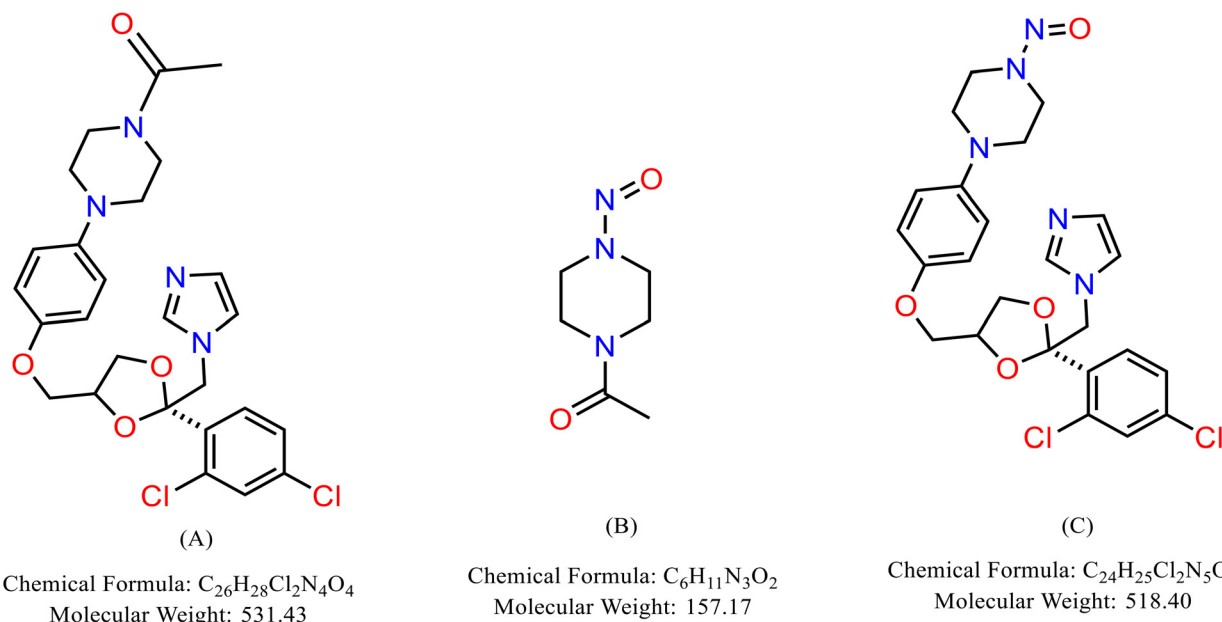


Fig. 1 Chemical structures of (A) KCZ API, (B) N-NAP, and (C) KCZ-degradant NDSRI.

supports global health and safety but also advances sustainable innovation in pharmaceutical analysis.

## 2. Experimental section

### 2.1. Standards and reagents

The reference compounds, KCZ DS (purity 99.79%) and *N*-acetyl piperazine (NAP, purity 99.42%), were received as complimentary samples from M/S Synpure Laboratories (Telangana, Pragati Nagar, Hyderabad, INDIA). The synthesis and subsequent characterization of *N*-nitroso acetyl piperazine (N-NAP) and the KCZ-*N*-nitroso degradant were accomplished, with structural verification provided by NMR and MS spectra. All LC-MS grade-ammonium formate, formic acid, trifluoroacetic acid, acetonitrile, and methanol were procured from Honeywell (Mumbai, INDIA). The commercially available KCZ 2% cream formulation and three different brands of KCZ tablets with a strength of 200 mg were procured from a local pharmacy (Telangana, Pragati Nagar, Hyderabad, INDIA).

### 2.2. Analytical instrumentation and software tools

A Waters Xevo TQ-XS MS system was utilized for the MRM analysis. The Waters Acquity H-Class UPLC system, featuring a sample manager with Flow Through Needle (FTN), quaternary solvent manager (QSM), TUV/PDA detector, and column manager with eCord (Waters Corporation, Milford, Massachusetts), was utilized. NMR spectra were obtained using a Bruker Avance-III NMR spectrometer, which features an Ascend 500 MHz magnet with a broadband observe (BBO) probe functioning at a temperature of 25 °C (Bruker, Billerica, Massachusetts). The impurity standards were weighed on an analytical balance (Mettler-Toledo (Columbus, Ohio);

Model: XPE205). For the analysis, high-purity water from the Millipore Milli-Q purification system (Bedford, MA) was used. The centrifuge used was an Eppendorf model 5810R (Hamburg, Germany). Millipore Millex-GV hydrophilic PVDF 0.22 µm filters were sourced from Millipore (Burlington, Massachusetts).

The molecular structures of KCZ and KCZ NDSRIs were drawn using PerkinElmer ChemDraw (Level: professional, v15.0.0.106). Two main (Q)-SAR methods were used: certified Derek Nexus (version 6.2.1, Knowledge: Derek KB 2022 2.0, Knowledge Date: January 6, 2022) and Sarah Nexus (version 3.2.1, Nexus: 2.5.1, Model: Sarah Model 2022.2). These tools were applied to evaluate mutagenicity, with bacteria as the test species and *in vitro* mutagenicity as the endpoint. NMR acquisition and processing parameters were handled using the TopSpin software, version 4.4. MassLynx and TargetLynx (v 4.2, SCN 1045) were used to manage the acquisition and processing parameters of the LC and MS.

### 2.3. Mobile phase solution preparation

Mobile phase A was prepared by diluting 1.0 mL of formic acid in 1000 mL of water, and mobile phase B was acetonitrile; both phases were degassed by ultrasonication.

### 2.4. Impurity standard preparation

N-NAP and KCZ-degradant NDSRIs were dissolved separately in a 70 : 30 (v/v) mixture of acetonitrile and 0.1% formic acid in water to obtain 1000 ng mL<sup>-1</sup> stock solutions.

### 2.5. KCZ-API sample preparation

A stock solution of KCZ API (10 mg mL<sup>-1</sup>) was prepared by accurately weighing ~100 mg of API into a 10 mL volumetric



flask, dissolving it in 5 mL diluent, sonicating for 15 min, and adjusting the volume with diluent at room temperature. The solution was filtered through a 0.22  $\mu\text{m}$  PVDF syringe filter.

## 2.6. KCZ-tablet formulation sample preparation

Ten tablets from three commercial brands were powdered using a mortar and pestle. An equivalent of 100 mg was transferred into a 20 mL Falcon tube, suspended in 10 mL diluent, sonicated for 15 min, and centrifuged at 3725g for 10 min. The supernatant was filtered through a 0.22  $\mu\text{m}$  PVDF syringe filter.

## 2.7. KCZ-cream formulation sample preparation

An equivalent of 100 mg KCZ (2% cream) was dispersed in 10 mL diluent, sonicated for 15 min, and centrifuged at 3725g for 10 min. The clear supernatant was filtered through a 0.22  $\mu\text{m}$  PVDF syringe filter.

## 3. Results and discussion

Owing to the lack of commercial and pharmacopeial standards for *N*-NAP and *N*-nitroso KCZ degradants, we synthesized and characterized these compounds using advanced spectroscopic techniques.

### 3.1. Synthesis and structural confirmation of KCZ degradation impurity (compound 1)

As per the available literature,<sup>31,32</sup> the KCZ degradation impurity was synthesized, and its structure was confirmed.

KCZ-API (1.0 g, approx. 1.9 mmol) was dissolved in 20 mL of 1 M HCl and heated under reflux at 80 °C for 4 hours. The reaction progress was monitored using thin-layer chromatography (TLC). After completion, the mixture was cooled to room temperature and neutralized with 1 M NaOH to pH ~7. The solution was then extracted with ethyl acetate (3  $\times$  20 mL), and the combined organic layers were dried over anhydrous Na<sub>2</sub>SO<sub>4</sub>, filtered, and concentrated. The synthetic scheme is shown in Fig. 2A.

Compound 1: Yield-95%; ESI-MS [M + H]<sup>+</sup> 489.39. <sup>1</sup>H-NMR (500 MHz, DMSO-d6):  $\delta$ (ppm) 7.69 (d, *J* = 2 Hz, 1H), 7.58 (d, *J* = 8.5 Hz, 1H), 7.48 (s, 1H), 7.44 (dd, *J* = 2, 8.5 Hz, 1H), 7.02 (s, 1H), 6.86 (m, 2H), 6.82 (s, 1H), 6.76 (m, 1H), 4.57 (dd, *J* = 45, 6 Hz, 2H), 4.33 (q, 1H), 3.85 (dd, *J* = 6.5, 7 Hz, 1H), 3.64 (m, 2H), 3.50 (dd, *J* = 5, 5.5 Hz, 1H), 2.91 (t, *J* = 5 Hz, 4H), 2.81 (t, *J* = 5 Hz, 4H) (Fig. S1).

### 3.2. General procedure for the synthesis of both *N*-nitroso compounds

A solution of compounds 1 and 2 (*N*-acetyl piperazine) (1.0 eq. each) in THF (10 mL) was cooled to 0 °C and stirred. To this, aqueous NaNO<sub>2</sub> (1.2 eq., 5 mL) was added dropwise, followed by AcOH (1.0 eq.). After stirring at RT for 12 h, the mixture was diluted with ice water and extracted with EtOAc. The combined organic layers were dried over Na<sub>2</sub>SO<sub>4</sub> and chromatographed

on silica gel (EtOAc/hexane) to afford *N*-nitroso derivatives 1a–2a. The synthetic scheme is shown in Fig. 2B.

#### 3.2.1. Structural characterization of *N*-nitroso KCZ degradant.

Compound 1a: yield-85%; ESI-MS [M + H]<sup>+</sup> 518.12. <sup>1</sup>H-NMR (500 MHz, DMSO-d6):  $\delta$ (ppm) 7.69 (d, *J* = 2 Hz, 1H), 7.58 (d, *J* = 8.5 Hz, 1H), 7.48 (s, 1H), 7.44 (dd, *J* = 2, 8.5 Hz, 1H), 7.02 (s, 1H), 6.97 (m, 2H), 6.82 (m, 2H), 6.80 (s, 1H), 4.53 (dd, *J* = 45, 6 Hz, 2H), 4.33 (m, 3H), 3.86 (m, 3H), 3.66 (m, 1H), 3.64 (dd, *J* = 5, 5.5 Hz, 1H), 3.54 (dd, *J* = 5, 5.5 Hz, 1H), 2.29 (t, *J* = 5 Hz, 4H), 3.09 (t, *J* = 5 Hz, 4H) (Fig. S2).

3.2.2. Structural characterization of *N*-NAP. Compound 2a: yield-93%; ESI-MS [M + H]<sup>+</sup> 158.01. <sup>1</sup>H-NMR (500 MHz, DMSO-d6):  $\delta$ (ppm) 4.30 (t, *J* = 5 Hz, 1H), 4.21 (t, *J* = 5 Hz, 1H), 3.77 (t, *J* = 5 Hz, 1H), 3.68 (m, 3H), 3.49 (m, 2H), 2.06 (d, *J* = 9.5 Hz, 3H) (Fig. S3).

Since no signals attributable to the nitroso group were observed in the standard <sup>1</sup>H or <sup>13</sup>C NMR spectra, more sophisticated spectroscopic tools were utilized to confirm its presence. Specifically, 2D <sup>15</sup>N-<sup>1</sup>H HMBC (heteronuclear multiple bond correlation) spectroscopy was used, which allowed for the detection of interactions between nitrogen and hydrogen atoms across multiple bonds. The spectra displayed clear long-range <sup>15</sup>N-<sup>1</sup>H correlations, providing conclusive evidence for the incorporation of the nitroso group into the molecular framework of both KCZ-NDSRIs (Fig. 3).

### 3.3. Establishing an interim control threshold for KCZ-degradant NDSRIs via CPCa (carcinogenic potency categorization approach) methodology

To overcome the challenges associated with establishing acceptable intake (AI) limits for nitrosamines, the EMA introduced the CPCa in July 2023. This approach categorizes nitrosamines based on their carcinogenic potency, facilitating AI determination, particularly in cases where compound-specific toxicological data are limited. NDSRI compounds are classified according to their  $\alpha$ -hydrogen count and assigned to one of five potency categories, each associated with an AI value between 18 and 1500 ng day<sup>-1</sup>.

The structural assessment of the identified NDSRIs indicated that both the *N*-NAP and the *N*-nitroso KCZ degradant possess two  $\alpha$ -hydrogens each (2,2). With reference to the CPCa scoring system, these impurities were assigned potency scores of 3. Consequently, both were classified under CPCa potency category 3, which denotes a comparatively lower carcinogenic concern relative to categories 1 and 2. A detailed summary of the categorization outcomes for KCZ-related NDSRIs is presented in Fig. 4. To establish an acceptable interim control limit for these impurities, the CPCa-recommended equation was applied, wherein the control limit (ppm) is derived from the ratio of the acceptable intake (AI, expressed in ng day<sup>-1</sup>) to the maximum daily dose (MDD, expressed in mg) of the drug substance. For ketoconazole, an MDD of 400 mg was considered. On this basis, the calculated interim control limit corresponds to <1  $\mu\text{g g}^{-1}$  (equivalent to 400 ng 400 mg<sup>-1</sup>). This specification defines a scientifically



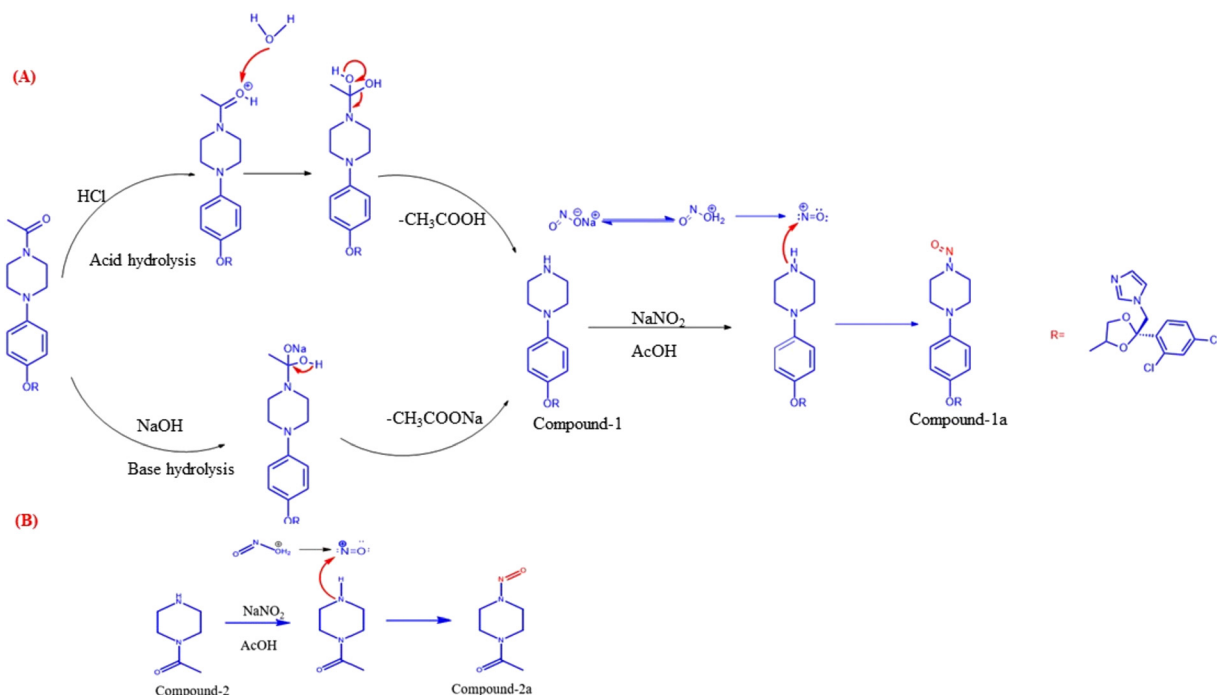


Fig. 2 Synthetic scheme of (A) KCZ-degradant NDSRI and (B) N-NAP.

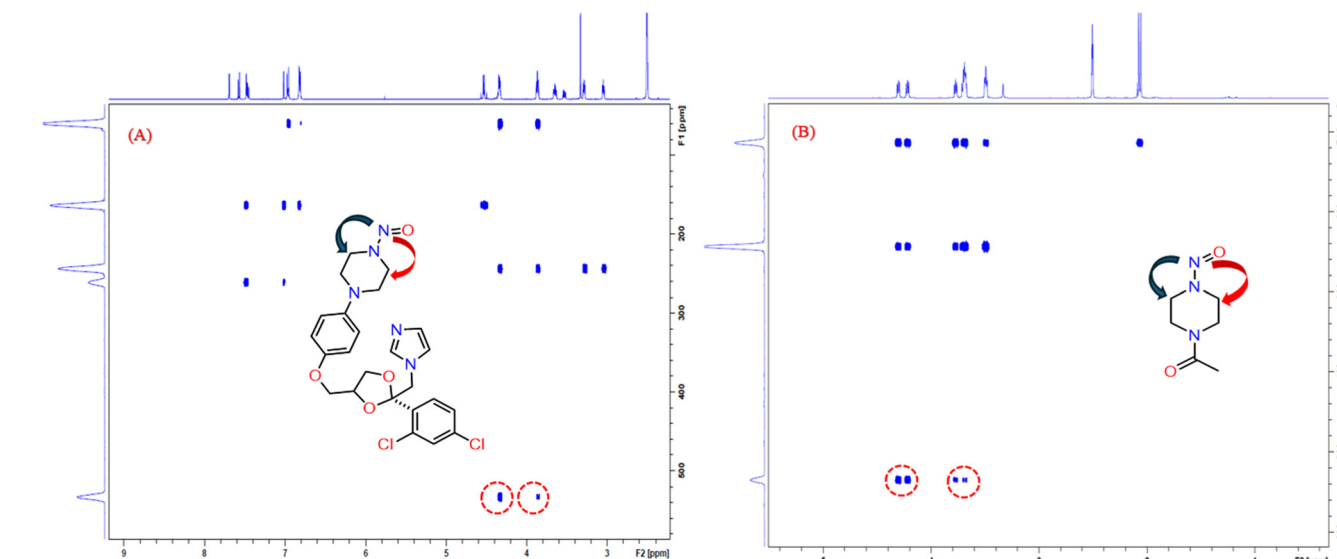


Fig. 3  $^1\text{H}$ - $^{15}\text{N}$  HMBC NMR spectra of (A) KCZ-degradant NDSRI and (B) N-NAP.

supported threshold consistent with regulatory guidance to safeguard patient safety.

### 3.4. (Q)-SAR data prediction

The (Q)-SAR approach plays a crucial role in regulatory decision-making by efficiently classifying chemical substances into predefined risk categories (ICH M7(R2) guideline).<sup>33</sup> It enables the rapid identification of potentially hazardous compounds, thereby supporting safety evaluations and ensuring

regulatory compliance in pharmaceutical development. KCZ, N-NAP, and KCZ-degradant NDSRIs were submitted using DEREK software, and the ICH classification model was employed to generate predictions. The anticipated results, summarized in Table 2, reveal that both statistical and expert rule-based (Q)-SAR predictions for NDSRIs were positive, classifying them as Class 3 and indicating potential mutagenicity. The integration of computational (Q)-SAR tools with CPCAguided potency categorization and specification limit determi-

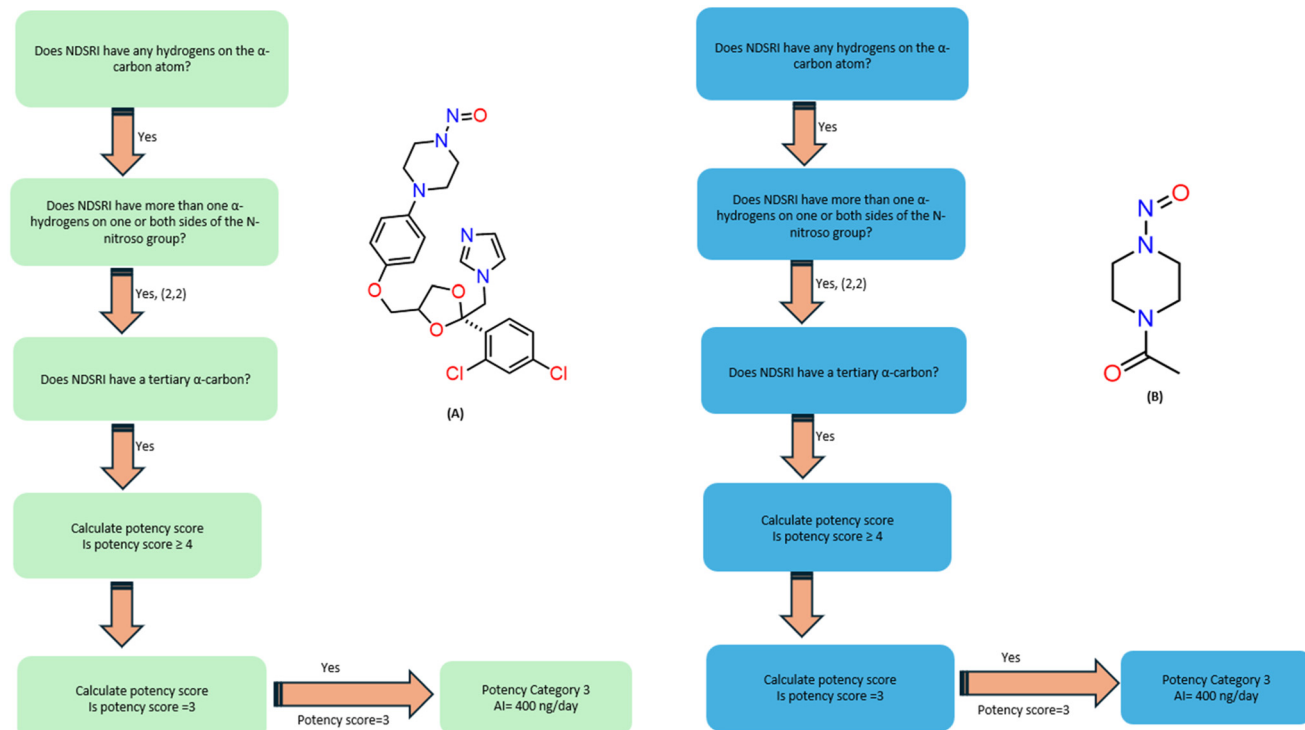


Fig. 4 Flow chart of the CPC approach for (A) KCZ-degradant NDSRI and (B) N-NAP.

Table 2 Summary of genotoxicity/mutagenicity assessment using the (Q)-SAR DEREK software

Structure	ICH M7 class	Coherent of concern	Derek prediction	Sarah prediction	Experimental data	Similar to API	Overall in silico
	Class-3	Yes (N-nitroso compound)			Carc: unspecified Ames: unspecified	Alert(s) not found in API	Positive
	Class-3	Yes (N-nitroso compound)			Carc: unspecified Ames: unspecified	Alert(s) not found in API	Positive

nation for KCZ-NDSRIs represents a critical advancement in promoting a more scientifically robust framework for pharmaceutical risk assessment. These efforts contribute directly to

achieving SDG 3, particularly Targets 3.8 and 3.d, by supporting universal access to safe medicines and enhancing health risk management capabilities.

### 3.5. Analytical target profile (ATP)

Adhering to the principles outlined in the ICH Q14 guideline,<sup>34</sup> the development of the analytical procedure prioritized defining the Analytical Target Profile (ATP), which was supported by effective knowledge management practices and comprehensive risk assessment to facilitate method understanding and control. The ATP defines the method's goals and criteria, ensuring consistent, accurate, and precise measurement while meeting regulatory standards throughout the product lifecycle.<sup>35</sup> The ATP connects quality objectives and analytical methods, enabling science-driven decisions from development to submission.

The primary objective of this investigation was to quantify trace levels of KCZ-degradant NDSRIs using state-of-the-art, highly sensitive detection techniques. Multiple Reaction Monitoring (MRM), a technique known for its exceptional specificity and sensitivity, was employed due to its application in drug development workflows. LC-TQ-MS/MS with MRM detection was implemented to analyze KCZ-NDSRIs in KCZ formulations. The sample preparation methodology was carefully modified based on the solubility profiles of the impurities, the KCZ API, and excipients to ensure efficient extraction and accurate chromatographic separation of the target NDSRIs. The proposed ATP for this investigation is outlined in Table 3.

### 3.6. Risk assessment and control strategy

To ensure analytical reliability, early-stage risk assessment addresses uncertainties, particularly matrix effects, by refining sample prep and instrumental controls. In this investigation, the effects were evaluated by adopting the quantifier-to-qualifier ion ratio (the ratio of the peak area of a qualifier ion to that of the quantifier ion for a given analyte-Q-to-*q* ratio) strategy in accordance with ICH Q2(R2).

The average ratio was calculated from six independently prepared calibration standards. The following expression was applied to estimate the deviation of the Q-to-*q* ratio for individual sample solutions:<sup>36</sup>

$$\begin{aligned} \text{Q-to-}q \text{ ratio deviation (\%)} \\ = \frac{(\text{average Q-to-}q \text{ ratio} - \text{sample Q-to-}q \text{ ratio})}{\text{average quantifier-to-qualifier ratio}} \times 100 \end{aligned}$$

### 3.7. Analytical procedure development and optimization

**3.7.1. Improving the sample preparation process and filter evaluation study.** Reliable trace-level analysis depends on optimized sample prep due to matrix effects. KCZ's solubility is influenced by pH and temperature; it is insoluble in water but soluble in methanol and methylene chloride.<sup>37</sup> After testing various concentration compositions, a 20 : 80 v/v mix of 0.1% formic acid in water and acetonitrile was found optimal for dissolving KCZ and two NDSRIs at a 5 mg mL<sup>-1</sup> KCZ concentration. After evaluating a range of sonication durations, a 15 minute treatment was determined to be the most effective for the extraction of KCZ-degradant NDSRIs. This extraction time consistently yielded recoveries exceeding 98%, indicating

Table 3 Analytical target profile (ATP)

Performance characteristics	Acceptance criteria	Rationale
Specificity	Absence of interference in the blank sample matrix Q to <i>q</i> ratio for test samples within ±20% tolerance	The general recommendation by the ICH Q2 and Q14 guidelines Recommendation in ICH Q2(R2)
Sensitivity Matrix effect	The quantitation limit (QL) of 1 µg g <sup>-1</sup> Q-to- <i>q</i> ratio for test samples within ±20% tolerance	The proposed necessitated the QL of 1 µg g <sup>-1</sup> Recommendation in ICH Q2(R2)
Accuracy	80%–120% CV ≤ 10 for QL limit	The general recommendation by the ICH Q2 and Q14 guidelines
Precision	0.06–1.5 µg g <sup>-1</sup> for N-NPA 0.1–1.5 µg g <sup>-1</sup> for KCZ-degradant-NDSRI	The general recommendation by the ICH Q2 and Q14 guidelines The AI value is 400; the interim control limit for KCZ-NDSRIs is 1 µg g <sup>-1</sup> (AI/MDD = 400 ng/400 mg)
Report range		



efficient and reproducible analyte release under these conditions. To further ensure the stability of the analytes during sample preparation, extended sonication periods beyond 15 minutes were also investigated. These additional tests revealed no signs of analyte degradation, confirming that the compounds remain stable even under prolonged ultrasonic exposure. In addition, a filter evaluation study was conducted to assess the potential analyte retention by the filtration material. Comparative analysis of KCZ solutions—both unfiltered and those subjected to centrifugation prior to filtration—revealed no significant differences in peak areas. The obtained results confirm the absence of adsorption of KCZ and its NDSRIs on the Durapore 0.22  $\mu\text{m}$  PVDF membrane filter, thereby validating its reliability for sample preparation, with no compromise in analyte recovery.

**3.7.2. Chromatographic separation method development.** The primary aim of this work is to develop a simple but reliable LC-TQ-MS/MS method that could identify and quantify trace levels of KCZ degradant-related nitrosamines (NDSRIs) in both the active pharmaceutical ingredient and finished formulations. To build a stable and sensitive method, we focused on carefully adjusting both the chromatographic and mass spectrometric parameters. Successful LC-MS method development requires consideration of multiple factors, including the physicochemical properties of the analytes, type and composition of buffer, stationary and mobile phases, column chemistry, temperature control, flow rate, gradient program or isocratic mode, injection volume, and the concentration of standards and samples. Each of these variables plays a role in achieving good resolution, sharp peak shapes, and reproducible quantification.

For the initial experiments, a 1 mg  $\text{mL}^{-1}$  mixed solution of KCZ and its degradant NDSRIs was prepared and injected. To prevent MS source contamination during method optimization, the LC effluent was initially diverted to waste. A systematic exploration of different mobile phase compositions and column chemistries was carried out. The main objective was to reduce peak broadening and improve the separation efficiency between KCZ and its degradant-NDSRI impurities.

Different reversed-phase C18 columns of varying dimensions and particle sizes were tested. In parallel, several volatile buffer systems were screened, including 0.1% trifluoroacetic acid (TFA), 10 mM ammonium acetate ( $\text{NH}_4\text{OAc}$ ), and 0.1% formic acid (FA) in acetonitrile/methanol. Initial trials using an Agilent Porosil C18 column (150  $\times$  4.6 mm, 2.7  $\mu\text{m}$ ) with mobile phases of  $\text{NH}_4\text{OAc}$  (10 mM), FA (0.1%), and TFA (0.1%) at a flow rate of 0.4  $\text{mL min}^{-1}$  and 40  $^\circ\text{C}$  column temperature resulted in poor chromatographic performance. Distorted peak shapes and co-elution of KCZ with its NDSRI degradants were observed under a linear gradient starting at 30 : 70 (v/v). Subsequently, a Waters Cortecs T3 C18 column (100  $\times$  4.6 mm, 2.7  $\mu\text{m}$ ) was evaluated under similar buffer and gradient conditions. However, this column caused very early elution of analytes, leading to co-elution of KCZ and *N*-NAP. The Waters XBridge BEH C18 column provided better performance. Early experiments on this column using 0.1% formic acid in aceto-

nitrile gave acceptable peak shapes and modest separation of KCZ and its NDSRI degradants. Further optimization of the gradient program significantly improved resolution, achieving excellent separation between KCZ, *N*-NAP, and KCZ-degradant NDSRI. Column temperature plays a critical role in LC-MS/MS by influencing analyte retention, peak shape, and method reproducibility. Fluctuations in temperature can lead to shifts in retention time, which is especially problematic in MRM-based methods, where detection is time-sensitive. The column temperature was optimized at 40  $^\circ\text{C}$  to achieve a balance between retention time stability, peak shape, and resolution. This systematic optimization of column chemistry, buffer type, and gradient program ultimately yielded a robust and reproducible LC-TQ-MS/MS method that can accurately detect and quantify trace levels of *N*-NAP and KCZ-degradant NDSRI. The retention times of *N*-NAP, KCZ, and KCZ-degradant NDSRIs are 3.72 min, 5.62 min, and 7.45 min, respectively (Fig. S4). The final chromatographic optimized conditions are shown in Table 4.

### 3.8. Optimization of MS/MS parameters

To enable the sensitive and selective quantification of KCZ-NDSRIs, a multiple reaction monitoring (MRM) method was developed using electrospray ionization (ESI) in positive ion mode. MRM is widely recognized owing to its ability to quantify compounds at trace levels, often in the nanogram per millilitre ( $\text{ng mL}^{-1}$ ) range, making it suitable for the analysis of low-abundance impurities, such as NDSRIs, in pharma-

**Table 4** Optimized UPLC chromatographic conditions

Parameter	Details
<b>UPLC conditions</b>	
Separation mode	Reversed phase
Instrument	Waters H-Class UPLC (Waters Corporation, USA) Auto sampler manager with a flow-through needle (FTN-L20FTP352G) Quaternary solvent manager (QSM-L20QSP358A) PDA-photo diode array detector model (L20UPD127A)
Column	Waters XBridge column (BEH C18-150 mm $\times$ 2.1 mm, 2.5 $\mu\text{m}$ )
Flow mode	Gradient
MP-A	0.1% FA in water
MP-B	Acetonitrile
Flow rate	0.4 mL/min
Needle wash	Acetonitrile : water (80 : 20) v/v
	Time (min)
Gradient program	
	0.0
	2.0
	8.0
	10.0
	10.1
	12.0
Column oven temperature	40 $^\circ\text{C}$
Sample cooler temperature	25 $^\circ\text{C}$
Injection volume	10.0 $\mu\text{L}$
Wavelength	230 nm
Run time	12.0 min



ceutical matrices. In this study, optimization of key mass spectrometric (MS) source parameters was essential to achieve robust ionization and a reproducible signal response. The source temperature was adjusted to facilitate efficient solvent evaporation, while the capillary voltage (CV) was optimized to promote the formation of charged droplets at the electrospray tip. In addition, the desolvation temperature (DT) and desolvation gas flow (DGF) were fine-tuned to assist in droplet drying and maintain spray stability. Under low-flow LC conditions, optimal values were established at 450 °C for DT and 850 L h<sup>-1</sup> for DGF, which consistently yielded strong and stable ion signals.

Initial tuning of the MS conditions was performed by direct infusion of a 1000 ng mL<sup>-1</sup> mixture of KCZ-NDSRIs. This allowed the identification of high-abundance precursor ions under positive ESI at a capillary voltage of 3.15 kV. Individual CV and collision energy (CE) values were then optimized for each target analyte. For *N*-NAP, three significant transitions were identified: *m/z* 158.01 → 55.87, 68.95, and 128.03. Similarly, for the KCZ-degradant NDSRI, three high-response transitions were observed: *m/z* 518.11 → 82.02, 445.18, and 459.15. Among these, the most intense and selective transitions were selected for quantitative analysis.

Dwell time—the duration the mass spectrometer monitors each MRM transition—is critical for balancing signal sensitivity and adequate data point coverage across chromatographic peaks. In LC-TQ-MS/MS methods with multiple transitions, improper dwell settings can compromise signal intensity and peak shape. Therefore, optimizing dwell time is essential in developing a reliable method for detecting KCZ-degradant NDSRIs and *N*-NPA. To improve the detection of KCZ-degradant NDSRIs, dwell time was systematically optimized. A dwell time of 50 ms was selected as optimal, providing clear, sharp peaks and reproducible quantification. The final MRM transitions used were *m/z* 158.01 → 68.95 (quantifier) and 158.01 → 128.03 (qualifier) for *N*-NAP, and *m/z* 518.11 → 459.15 (quantifier) and 518.11 → 82.02 (qualifier) for the KCZ-degradant NDSRI. To further improve method specificity and minimize matrix-related interferences from KCZ drug substance and cream formulation samples, a time-segmented flow switching strategy was implemented. From 0.00 to 5.00 minutes, the LC flow was directed to the MS to detect *N*-NAP. Between 5.00 and 6.50 minutes, the flow was diverted to waste to prevent potential contamination from the formulation components. Subsequently, from 6.53 to 12.00 minutes, the flow was rerouted to the MS to detect KCZ-degradant NDSRIs. This dynamic flow control approach effectively reduced background noise and ensured high-quality, reproducible data, supporting the applicability of the method for the routine analysis of nitrosamine impurities in complex pharmaceutical matrices. Needle wash is a critical step in LC-MS/MS methods for preventing sample carryover and contamination between injections, especially for nitrosamine impurity quantification. Inadequate needle washing can lead to false positives, inaccurate quantification, and poor reproducibility. Optimizing the needle wash solvent and duration effectively

removes the residual samples from the needle and seat, minimizing the carryover, which is crucial for trace-level or variable concentration analyses. To prevent this, the needle wash step was optimized by testing different acetonitrile–water ratios. An 80 : 20 (v/v) mixture proved to be the most effective in minimizing contamination. The optimized transitions, along with the detailed MS parameters, are provided in Fig. S5 and Table 5.

### 3.9. Robustness study

According to the ICH Q2(R2) guidelines,<sup>38</sup> robustness is a critical aspect of method development that ensures reliable and consistent performance when experimental conditions are varied. The robustness of the method was evaluated by examining its performance under slight variations under chromatographic and MS conditions, following the guidelines outlined in ICH Q2(R2). Parameters such as flow rate, column temperature, DT, CE, and DGF were deliberately altered. Even under these conditions, the method showed consistent performance, with variation in KCZ-NDSRIs content under <10%, confirming its robustness (Table S1).

### 3.10. Projected established conditions (ECs) and reporting categories

According to ICH Q12,<sup>39</sup> ECs are key aspects of analytical procedures that require appropriate control to ensure reliable and reproducible performance. These include factors like column type, mobile phase, flow rate, detection wavelength, and system suitability. Changes to ECs usually require regulatory approval. Defining ECs supports method robustness and regulatory compliance throughout the method lifecycle. Table 6 summarizes the projected ECs along with their corresponding ICH Q12 reporting categories for the proposed LC-TQ-MS/MS method used in the detection and quantification of KCZ-NDSRIs.

### 3.11. Analytical method validation study

The optimized LC-TQ-MS/MS method was thoroughly validated following ICH Q2(R2) guidelines, USP General Chapter <1469><sup>40</sup> guideline and established literature,<sup>41–46</sup> confirming its specificity, both method and intermediate precision, detection and quantification limits (DL and QL), linearity and accuracy.

**3.11.1 Sensitivity/system suitability test (SST) solution.** SST was verified prior to initiating the validation parameters. A 5 ng mL<sup>-1</sup> SST solution of each *N*-NAP and KCZ degradant NDSRI was injected in six replicates. Precision was evaluated *via* peak area and retention time, with all CVs maintained under 5%. Sensitivity was assessed using signal-to-noise ratios (minimum S/N ≥10). The results indicated CVs of 1.39% for *N*-NAP and 1.12% for KCZ-degradant NDSRI, with corresponding S/N values of 84 and 61, respectively.

**3.11.2. Specificity.** The method's specificity was evaluated by individually injecting placebo, diluent, and standard solutions containing 10 ng mL<sup>-1</sup> of each *N*-NAP and *N*-nitroso KCZ-degradant, followed by a spiked cream formulation sample (10 mg mL<sup>-1</sup>) fortified with 10 ng mL<sup>-1</sup> of each



**Table 5** Finalized tuning MRM mass spectrometry conditions for KCZ-NDSRIs in the ESI<sup>+ve</sup> mode

Compound	Chemical formula	Precursor ion ( <i>m/z</i> )	Product ion ( <i>m/z</i> )	Spectral window (min)	Dwell time (ms)	Collision energy (V)	Cone voltage (V)
<i>N</i> -NPA	C <sub>6</sub> H <sub>11</sub> N <sub>3</sub> O <sub>2</sub>	158.01	68.95 (quantifier ion) 128.03 (qualifier ion)	3.45–3.93	50	6	18
KCZ-degradant NDSRIs	C <sub>24</sub> H <sub>25</sub> Cl <sub>2</sub> N <sub>5</sub> O <sub>4</sub>	518.11	459.154 (quantifier ion) 82.024 (Qualifier ion)	7.30–7.95	50	14	28

**Table 6** Established conditions (ECs)

Proposed ECs	Overall risk assessment	Proposed ICHQ12 reporting category	Rationale	Supporting data
Method	High	Prior approval (PA)	Analytical target profile Control strategy: <i>Q</i> -to- <i>q</i> ratio	LC-QQQ-MS/MS was the only analytical technology that demonstrated the sensitivity required by the ATP. Any change in the technological principle poses a high risk of sensitivity and other performance characteristics.
LC-QQ-MS/MS method				
Equipment	High	PA	Analytical target profile Control strategy: <i>Q</i> -to- <i>q</i> ratio	Triple quadrupole detection was chosen in development studies to meet the sensitivity requirements. Changing the detector type also introduces significant risks to other performance measures.
Triple quadrupole ESI <sup>+ve</sup> mode				
Conditions	High	PA	Analytical target profile Control strategy: <i>Q</i> -to- <i>q</i> ratio	Matrix effects resulting from changes in excipients, additives, and formulation parameters. In the current study, the Quantifier-qualifier ratio for standard and sample tolerance should be <20%
Internal standard not using				
Formation of adducts	High	PA	Analytical target profile Control strategy: <i>Q</i> -to- <i>q</i> ratio	During the development study, the ammonium adduct was observed while using ammonium acetate buffer, hence avoiding ammonium acetate usage.
Flow rate (mL min <sup>-1</sup> )	Low		NL (notification low), If within 0.2–0.3	The method robustness data (Table S1) demonstrate that the method performed adequately under the specified conditions.
Column temp. (°C)	Low		NL, if within 38–42	
Desolvation gas temp. (°C)	Low		NL, if within 400–500	
Desolvation gas flow (L/Hr)	Low		NL, if within 850–950	
Collision energy (V)	Medium		NL, if within 16–20	

KCZ-NDSRI. This assessment ensured that no extraneous or interfering peaks were observed at the respective retention times or target *m/z* values corresponding to the analytes of interest. Furthermore, the obtained *Q*-to-*q* ion ratios for each compound were found to be consistent with the reference standards, which remained within an acceptable deviation limit of  $\pm 20\%$ , thereby confirming the method's selectivity and reliability for accurate quantification in the presence of formulation excipients (Fig. 5).

**3.11.3. Estimation of the detection limit (DL) and quantitation limit (QL).** The DL and QL for *N*-NPA and KCZ-degradant NDSRIs were determined using a signal-to-noise ratio (S/N) of 3 for DL and 10 for QL by injecting standard solutions of known concentrations. The DL and QL values were found to be 0.2 and 0.6 ng mL<sup>-1</sup> for *N*-NPA and 0.3 and 1 ng mL<sup>-1</sup> for KCZ-degradant NDSRIs, respectively. The repeatability of the QL was determined by injecting the *N*-NPA and KCZ-degradant NDSRI impurities six times into the LC-TQ-MS/MS, and the %

CV was calculated, yielding 2.15% for *N*-NPA and 2.85% for KCZ-degradant NDSRIs (Table 7).

**3.11.4. Method precision and intermediate precision.** Method precision was evaluated by analyzing six replicate preparations of KCZ-DS and cream formulation at a concentration of 10 mg mL<sup>-1</sup>, spiked with nitrosamine impurities at the interim control limit (1  $\mu$ g g<sup>-1</sup>). Intermediate precision was assessed by reanalysing the same samples on a separate day using the same system. The developed method demonstrated excellent precision, with %CV values for both repeatability and intermediate precision remaining below 10% (Table 7).

**3.11.5. Linearity/calibration curve performance.** The optimized method was evaluated for linearity over the range of 1–15 ng mL<sup>-1</sup> (equivalent to 0.1–1.5  $\mu$ g g<sup>-1</sup> for a 10 mg mL<sup>-1</sup> KCZ sample). Calibration curves were constructed by plotting peak areas against concentrations at seven levels using a  $1 \times 1$  weighting for the range of 1–15 ng mL<sup>-1</sup>. The slope (*a*), inter-



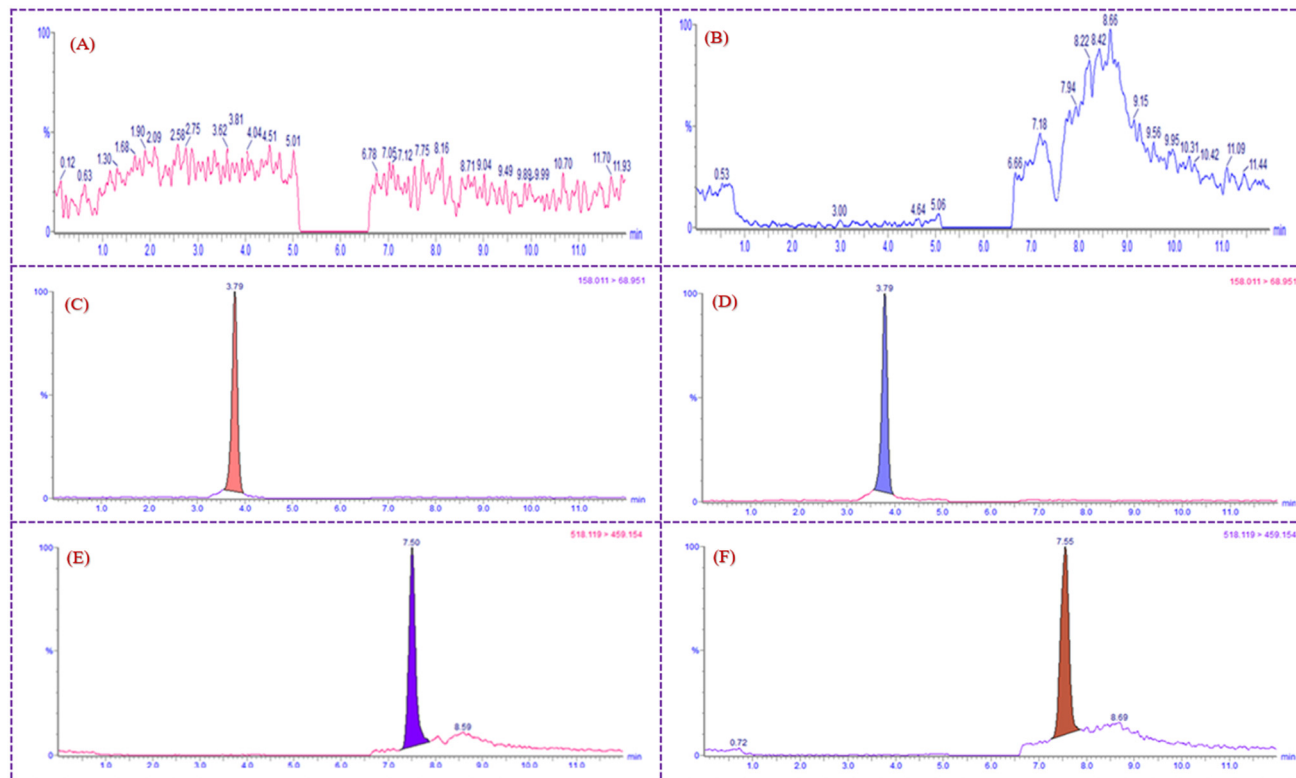


**Fig. 5** Typical MRM chromatograms of (A) diluent, (B) placebo, (C)  $10 \text{ ng mL}^{-1}$  of standard N-NAP, (D) spiked  $10 \text{ ng mL}^{-1}$  of N-NAP in a cream formulation at  $10 \text{ mg mL}^{-1}$  of sample concentration, (E)  $10 \text{ ng mL}^{-1}$  of standard KCZ-degradant NDSRI, and (F) spiked  $10 \text{ ng mL}^{-1}$  of KCZ-degradant NDSRI in a cream formulation at  $10 \text{ mg mL}^{-1}$  of sample concentration.

cept (b), and Pearson correlation coefficient ( $r$ ) were determined *via* least squares linear regression, yielding the following equations:  $Y = 993.12X + 163.925$  for N-NPA and  $Y = 1422.02X - 909.34$  for KCZ-degradant NDSRI. To confirm the validity of the calibration, back-fit bias was calculated at each concentration level, with all values falling within the acceptable range of  $\pm 10\%$ , demonstrating accuracy. As summarized in Table 7, a strong correlation was observed between the peak areas and the concentrations of nitrosamine impurities, confirming the method's linear response across the tested range.

**3.11.6. Matrix effects.** In this study, the influence of the matrix effect (ME) on the analytical performance of the method was systematically evaluated. The assessment was conducted by comparing the slopes of the calibration curves constructed in both the sample matrix and the solvent medium. This approach enables the identification of any signal enhancement or suppression arising from matrix constituents that may interfere with analyte ionization or detection. A slope ratio between 0.85 and 1.15 was interpreted as indicative of an insignificant matrix effect, suggesting that the matrix components exerted minimal influence on the analytical signal and overall quantification accuracy.<sup>47</sup> For this evaluation, the KCZ-cream formulation extraction solution was employed as the representative matrix for the actual sample. A slope ratio of 0.94 indicated negligible matrix interference, with no signal suppression or enhancement observed. Therefore, the matrix

exhibited minimal influence on analyte ionization, confirming that the method is consistent and reliable.

**3.11.7. Accuracy/recovery study.** The accuracy of the optimized method was evaluated using the standard addition method, which entailed spiking DS and 2% cream formulation samples of KCZ at three distinct concentration levels:  $0.06 \mu\text{g g}^{-1}$  (QL),  $1 \mu\text{g g}^{-1}$  (100%), and  $1.5 \mu\text{g g}^{-1}$  (150%) for N-NPA, and  $0.1 \mu\text{g g}^{-1}$  (QL),  $1 \mu\text{g g}^{-1}$  (100%), and  $1.5 \mu\text{g g}^{-1}$  (150%) for KCZ-degradant-NDSRI. This evaluation was performed in triplicate determinations for each concentration level to ensure reproducibility and reliability. The mean recoveries for each level and each nitrosamine impurity were calculated, and the mean recoveries for N-NPA were obtained from 96.85 to 101.15%, and 94.12 to 100.02% in KCZ-DS and 2% cream formulations, respectively. The KCZ-degradant-NDSRIs ranged from 96.02% to 101.02% and 95.15% to 100.45% in the KCZ-DS and 2% cream formulations, respectively. These recovery ranges are within acceptable limits, confirming that the method is accurate across the tested concentration levels. The detailed accuracy results are presented in Table 7.

**3.11.8. Solution stability.** Stability of the N-NAP and KCZ-degradant NDSRI impurity in solution was demonstrated by spiking both pure and formulated KCZ products at 1.0 ppm, storing them under ambient conditions, and performing repeated analysis at different time intervals from 0 to 24 h. Each solution was analysed in triplicate using the validated

Table 7 Summary of the method validation results

Method validation parameter	Sample and procedure	Target criteria	Results	
			N-NPA	KCZ-degradant NDSRI
Specificity	Diluent, placebo, standard solution, and sample solutions	No interference with peaks of interest	No interference	No interference
Precision	Three levels of spiked solutions (50%, 100%, and 150%) in triplicate injections	$Q\text{-}q$ deviation should be $\leq 20\%$ The % CV of the 6 recoveries is $\leq 20\%$	2.18 0.98	1.98 1.02
Intermediate precision	The same samples prepared for precision were used for analysis on a different day with the same instrument	% CV of the 6 recoveries is $\leq 20\%$ ; The % CV of the 12 recoveries is $\leq 25\%$	1.05 1.02	1.09 1.05
Detection limit (DL)		Signal-to-noise ratio (S/N) $\geq 3$	5.6	4.5
Quantitation limit (QL)		Signal-to-noise ratio (S/N) $\geq 10$	14.9	11.9
QL precision		The % CV of the 6 replications is $\leq 20\%$	2.15	2.85
Linearity	Range (ng mL <sup>-1</sup> )	Pearson coefficient $>0.99$	0.06–15 993.12 163.925 0.9999	1–15 1422.02 –909.34 0.9992
Recovery	For KCZ drug substance: The level at QL mean $\pm$ SD The level at 100% mean $\pm$ SD The level at 150% mean $\pm$ SD For KCZ cream formulations: The level at QL mean $\pm$ SD The level at 100% mean $\pm$ SD The level at 150% mean $\pm$ SD	The average recovery at each level is within 80%–120%	96.85 $\pm$ 0.85 99.95 $\pm$ 0.56 101.15 $\pm$ 0.28 94.12 $\pm$ 1.05 99.45 $\pm$ 1.05 100.02 $\pm$ 0.69	96.02 $\pm$ 1.59 100.08 $\pm$ 0.89 101.02 $\pm$ 1.25 95.15 $\pm$ 0.98 100.45 $\pm$ 0.59 99.49 $\pm$ 1.25
Solution stability		Peak area (0 h to 24 h, % difference with initial $<10$ for both nitrosamine impurities)	0.98	1.42

method, and the peak areas for both nitrosamine impurities were compared with those obtained from freshly prepared standard solutions. No significant changes in peak area ( $<10\%$  for both NDSRIs) were observed across all time points. These findings indicate that both nitrosamine impurities exhibit chemical stability in solution for a minimum of 24 h under the tested conditions, supporting the use of prepared standard and sample solutions within this timeframe for routine analytical purposes.

### 3.12. Real-time analysis of commercial KCZ tablets and cream formulations to demonstrate method applicability

Each nitrosamine impurity detected in the DS or DP must be quantified against its respective AI. In cases where more than one nitrosamine is present, their levels must be proportionally limited such that the total combined exposure does not exceed 100% of the permitted. To demonstrate applicability, three marketed KCZ formulations—200 mg tablets and 2% cream—were analysed using the proposed LC-TQ-MS/MS method. Triplicate injections of each sample showed no detectable KCZ-NDSRIs, indicating that the products met regulatory impurity limits (Fig. S6).

### 3.13. Environmental footprint analysis of the current validated LC-TQ-MS/MS procedure

The environmental sustainability of the anticipated LC-TQ-MS/MS method procedure was rigorously evaluated using estab-

lished literature<sup>48</sup> and cutting-edge green analytical chemistry assessment tools, including AGREE, MoGAPI, Mo Complex GAPI, BAGI, RAPI and CaFRI. These tools offer a robust and quantitative overview of the method's green credentials.

**3.13.1. AGREE (analytical GREENness) evaluation tool.** Pena-Pereira's AGREE tool<sup>49</sup> is a comprehensive software-based assessment system designed to evaluate the overall "greenness" of analytical procedures in accordance with GAC principles. It offers a holistic assessment by integrating all 12 GAC principles into a circular chart, with each segment representing one criterion. The tool generates a greenness score between 0 (least green) and 1 (most green), enabling easy comparison of analytical methods. In this study, the proposed method obtained an AGREE score of 0.72, placing it in the green zone and indicating strong compliance with GAC principles. This reflects its low environmental impact, efficient resource use, and minimal reliance on hazardous reagents (Fig. 6A and Table S2).

**3.13.2. MoGAPI assessment tool.** As an extension of the GAPI, MoGAPI<sup>50</sup> evaluates analytical methods in terms of environmental impact and safety using color-coded pictographic representations. The present method, using minimal energy,  $<10$  mL of low-hazard solvents, and generating minimal waste, scored 76—ranking as excellent green (Fig. 6B and Table S2).

**3.13.3. BAGI assessment tool.** The BAGI evaluation system<sup>51</sup> enhances green assessments by highlighting solvent



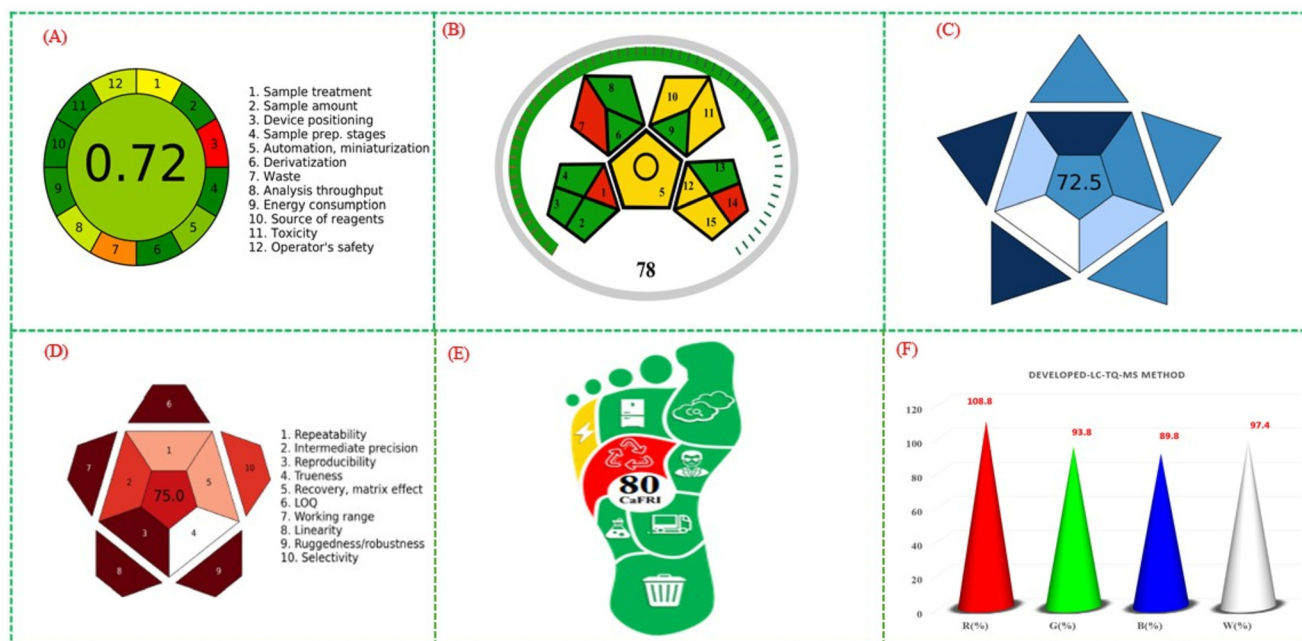


Fig. 6 Pictograms of (A) AGREE, (B) MoGAPI, (C) BAGI, (D) RAPI, (E) CaFRI, and (F) WAC.

safety, energy use, and waste reduction. It functions as the blue axis within the RGB system, scoring methods from 25 to 100 over ten assessment categories. The current LC-TQ-MS/MS analytical procedure achieved a score of 72.5, indicating good environmental sustainability (Fig. 6C).

**3.13.4. Red analytical performance index (RAPI) tool.** The RAPI tool<sup>52</sup> was used to evaluate and visualize the overall analytical performance of a method by focusing on analytical efficiency, reliability, and real-time analysis applicability rather than solely environmental or green aspects. The development of RAPI is rooted in the concept of White Analytical Chemistry (WAC) and aligns with the red element of the RGB model. RAPI offers a comprehensive performance assessment by examining factors like selectivity, sensitivity, accuracy, and precision. It further considers the detection limit, analytical time, economic viability, sample preparation complexity, instrument requirements, and overall reproducibility. The current analytical procedure performance score is 75, indicating a strong, acceptable performance (Fig. 6D).

**3.13.5. Carbon footprint reduction index (CaFRI) tool.** The CaFRI assessment tool<sup>53</sup> is designed to evaluate the environmental impression of analytical procedures by measuring their carbon footprints. It helps quantify how much greenhouse gas emissions (usually CO<sub>2</sub> equivalents) are associated with each step or component of an analytical procedure. This tool evaluates energy usage, CO<sub>2</sub> emission, sample storage and transportation, personnel, waste amount and disposal, recycling and amount usage of solvents/reagents. It is particularly valuable in areas focused on reducing environmental impact, including pharmaceutical analysis, environmental monitoring, and sustainability-driven quality control laboratories. The CaFRI scale ranges from 0 to 100, where lower scores (0–49) suggest poor

environmental efficiency, mid-range scores (50–74) indicate moderate sustainability, and higher scores (75–100) indicate excellent carbon footprint reduction. The current analytical procedure achieved a score of 80 (Fig. 6E), showing its excellent sustainability practices.

**3.13.6. Whiteness assessment tool RGB12 for the proposed LC-TQ-MS/MS method.** Nowak *et al.* (2021) proposed WAC as an advancement over the 12 principles of GAC, which aims at fostering safer and more sustainable analytical methodologies. The RGB12 Whiteness Assessment tool quantifies the overall sustainability of an analytical procedure by combining three color-coded groups: red, green, and blue. This work employs the RGB12 model to present a novel metric for evaluating NDSRI, merging sustainable development goals with analytical chemistry principles. The colors represent different attributes: red for analytical efficiency (R1–R4), green for environmental friendliness (G1–G4), and blue for economic viability (B1–B4). The WAC status classifies methods as poor white (0–25), average white (26–50), good white (51–75), excellent white (76–100), and extraordinary white (>100).<sup>54–58</sup>

The proposed LC-TQ-MS/MS analytical procedures achieved exceptional red color scores of 108.8% and 100%, signifying outstanding accuracy and precision in quantifying KCZ-NDSRI impurities. Furthermore, the method attained notable greenness scores (93.8%), indicating minimal environmental burden and adherence to eco-friendly analytical practices. The efficiency evaluation revealed blue scores of 89.8%, confirming their superior operational and economic performance. As shown in Table 8, the proposed LC-TQ-MS/MS method achieved an overall whiteness score of 97.4%, indicating an excellent white status (Fig. 6F).



**Table 8** WAC-based assessment of proposed LC-TQ-MS method using the RGB12 model

Principles of white analytical chemistry	Score
Red principles (analytical performance)	
R1: scope of application	LC-TQ-MS method 110
R2: DL and QL	DL: 0.2–0.3 ng mL <sup>-1</sup> 120 QL: 0.6–1 ng mL <sup>-1</sup>
R3: precision	Method precision ( $\leq 2\%$ ) 100 Intermediate precision ( $\leq 2\%$ )
R4: accuracy	Recovery (94%–101%) 105
Total average score	108.8
Green principles (green chemistry)	
G1: toxicity of reagents (impact and biodegradation)	Total number of pictograms-3 100
G2: amount of reagents and waste	Reagent consumption 100 Waste production (480 mL per 100 runs)
G3: consumption of energy and other media	LC-TQ-MS 75
G4: direct impacts (safety, use of animals and GMOs)	Occupational hazards 100 Safety of users Use of animals (0 if no, 1 if yes) Use of GMO (0 if no, 1 if yes)
Total average score	93.8
Blue principles (practical side)	
B1: cost-efficiency	Total cost 70
B2: time-efficiency	Speed of analysis 100
B3: requirements	Sample consumption (480 mL per 100 runs) 85 Other needs: advanced instruments, skills, and facilities (0–100) 100
B4: operational simplicity	Miniaturization 100 Integration and automation 100 Portability 100
Total average score	89.8
WAC score	Average of RGB score (108.8 + 93.8 + 89.8) 97.4
WAC status	Excellent white

## 4. Conclusion

The simple, eco-friendly, and highly sensitive LC-TQ-MS/MS method for the quantification of Ketoconazole-NDSRIs was optimized in the present study. Successfully synthesized *N*-nitroso impurities of Ketoconazole and the structures were confirmed using two-dimensional NMR spectroscopy (2D-NMR)  $^1\text{H}$ – $^{15}\text{N}$  HMBC spectra for both nitrosamine impurities. Acceptable intake values were determined using the carcinogenic potency categorization approach. This study effectively demonstrates the ICH Q14 analytical procedure development guidelines for the analytical target profile, and following the ICHQ2(R2) guidelines, the optimized method conditions were validated for linearity, DL, QL, accuracy, method precision, and intermediate precision. The optimized method showed excellent performance with higher recoveries and lower % CV values. The proposed LC-TQ-MS/MS method was successfully utilized for commercial KCZ tablet and cream formulations, demonstrating its adaptability in ensuring product quality and human safety. The green and whiteness of the proposed method was assessed using advanced tools, including AGREE, Modified GAPI, BAGI, RAPI CaFRI and RGB12. Overall, this

study provides a practical, sustainable, and regulatory-compliant approach for monitoring KCZ-NDSRIs, which aims at protecting human health.

## Author contributions

Srinivas Nakka: writing– original draft, validation, software, methodology, visualization, investigation, formal analysis, conceptualization. Vishnu Marisetti: review & editing, visualization, data curation. Surendra Babu Manabolu Surya: writing – review & editing, visualization, supervision, resources, project administration.

## Conflicts of interest

The authors declare that they have no known competing financial interests or personal relationships that could have appeared to influence the work reported in this paper.

## Data availability

All the experimental data are included in this study and the supplementary information (SI). Supplementary information is available. See DOI: <https://doi.org/10.1039/d5an01052g>.

## Acknowledgements

Sincere thanks to the Gitam University management.

## References

- 1 U. Holzgrabe, *J. Pharm. Sci.*, 2023, **112**, 1210–1215.
- 2 D. Aishwarya, V. R. Dhampalwar, N. Pallaprolu and R. Peraman, *Pharm. Res.*, 2025, **42**, 547–578.
- 3 M. J. Burns, D. J. Ponting, R. S. Foster, B. P. Thornton, N. E. Romero, G. F. Smith, R. J. Sperry and R. L. Hart, *J. Pharm. Sci.*, 2023, **112**, 3005–3011.
- 4 R. C. Cioc, C. Joyce, M. Mayr and R. N. Bream, *Org. Process Res. Dev.*, 2023, **27**, 1736–1750.
- 5 R. P. Adhikari, A. M. S. Tharik and S. N. Meyyanathan, *J. Chromatogr. Sci.*, 2022, **61**, 585–604.
- 6 M. Blessy, R. D. Patel, P. N. Prajapati and Y. Agrawal, *J. Pharm. Anal.*, 2013, **4**, 159–165.
- 7 W. Ashworth, A. Blanazs, J. J. Byrne, O. Dirat, J. W. Fennell, N. Kuhl, R. A. Storer, T. S. Moody and D. E. Herbert, *Org. Process Res. Dev.*, 2023, **27**, 1784–1791.
- 8 J. Wohlfart, F. Sörgel and U. Holzgrabe, *J. Pharm. Biomed. Anal.*, 2019, **172**, 278–284.
- 9 US FDA, *Laboratory analysis of valsartan products*, 2019. Available at: <https://www.fda.gov/drugs/drug-safety-and-availability/laboratory-analysis-valsartan-products> (accessed June 30, 2025).



10 US FDA, *Lupin Pharmaceuticals Inc issues voluntarily nationwide recall of all irbesartan tablets and irbesartan*, 2019. Available at: <https://www.fda.gov/safety/recalls-market-withdrawals-safety-alerts/lupin-pharmaceuticals-inc-issues-voluntarily-nationwide-recall-all-irbesartan-tablets> (accessed June 30, 2025).

11 L. Sridhar, P. Goutami, D. V. Darshan, K. Ramakrishna, R. N. Rao and S. Prabhakar, *Anal. Methods*, 2014, **6**, 8212–8221.

12 S. Arar, E. Al-Qudah, M. Alzweiri and K. Sweidan, *J. Liq. Chromatogr. Relat. Technol.*, 2020, **43**, 633–644.

13 P. Mital, K. Charmy and V. Vivek, *Arabian J. Chem.*, 2020, **13**, 6493–6509.

14 V. Malati, A. R. Reddy, K. Mukkanti and M. Suryanarayana, *Talanta*, 2012, **97**, 563–573.

15 P. Peng, C. Zhao, J. Yang, X. Liu, J. Yu and F. Zhang, *Org. Prep. Proced. Int.*, 2022, **54**, 203–219.

16 S. Nakka, N. K. Katari, S. K. Muchakayala and S. B. Jonnalagadda, *Talanta Open*, 2023, **7**, 100221.

17 S. Jadhav, P. Reddy, K. Narayanan and P. Bhosale, *Sci. Pharm.*, 2017, **85**, 25.

18 L. Pagano and O. M. Fernández, *J. Antimicrob. Chemother.*, 2025, **80**, i2–i8.

19 J. Maertens, *Clin. Microbiol. Infect.*, 2004, **10**, 1–10.

20 A. K. Gupta, D. Daigle and K. A. Foley, *Expert Opin. Drug Saf.*, 2014, **14**, 325–334.

21 F. D. Choi, M. L. Juhasz and N. A. Mesinkovska, *J. Dermatol. Treat.*, 2019, **30**, 760–771.

22 R. Pivonello, C. Simeoli, M. C. De Martino, A. Cozzolino, M. De Leo, D. Iacuaniello, C. Pivonello, M. Negri, M. T. Pellecchia, F. Iasevoli and A. Colao, *Front. Neurosci.*, 2015, **9**, 129.

23 Grand View Research, *Antifungal drugs market size, growth trends, share & forecast report, 2030*, 2023. Available at: <https://www.grandviewresearch.com/industry-analysis/antifungal-drugs-market> (accessed 30 June 2025).

24 R. A. Mhaske, *Sci. Pharm.*, 2011, **79**, 817–836.

25 W. Yang, X. Yang, F. Shi, Z. Liao, Y. Liang, L. Yu, R. Wang, Q. Li and K. Bi, *J. Pharm. Anal.*, 2019, **9**, 156–162.

26 S. K. Muchakayala, N. K. Katari, K. K. Saripella, V. M. Marisetti and L. P. Kowtharapu, *Sustainable Chem. Pharm.*, 2023, **36**, 101247.

27 N. Gaur, N. Parvez and K. Nagpal, *J. Appl. Spectrosc.*, 2025, **92**, 437–445.

28 P. T. Anastas and J. C. Warner, *Green Chemistry*, Oxford University Press, Oxford, 2000.

29 Z. Galuszka, Z. Migaszewski and J. Namieśnik, *TrAC, Trends Anal. Chem.*, 2013, **50**, 78–84.

30 United Nations, *Sustainable Development Goals (SDGs)*, 2025. Available at: <https://sdgs.un.org/goals> (accessed 2 July 2025).

31 O. Štěpánek, A. Čmoková, E. Procházková, V. Grobárová, J. Černý, M. Slapničková, A. Zíková, M. Kolařík and O. Baszczyński, *ChemMedChem*, 2022, **17**, e202200385.

32 M. Sasaki, K. Arashima, T. Nakanishi and H. Yamane, Office Sam Co. Ltd., JP2017105738A, 2017.

33 International Council for Harmonisation (ICH), ICH harmonised guideline M7(R2): Assessment and control of DNA reactive (mutagenic) impurities in pharmaceuticals to limit potential carcinogenic risk, April 2023. Available at: [https://database.ich.org/sites/default/files/ICH\\_M7R2\\_Guideline\\_2023\\_0321\\_1.pdf](https://database.ich.org/sites/default/files/ICH_M7R2_Guideline_2023_0321_1.pdf) (accessed 2 July 2025).

34 International Council for Harmonisation (ICH), ICH harmonised guideline Q14: Analytical procedure development, November 2023. Available at: [https://database.ich.org/sites/default/files/ICH\\_Q14\\_Guideline\\_2023\\_1116\\_1.pdf](https://database.ich.org/sites/default/files/ICH_Q14_Guideline_2023_1116_1.pdf) (accessed 2 July 2025).

35 M. K. Parr and A. H. Schmidt, *J. Pharm. Biomed. Anal.*, 2017, **147**, 506–517.

36 S. Nakka, S. K. Muchakayala and S. Manabolu, *Microchem. J.*, 2025, **214**, 114065.

37 S. Alshehri, A. Hussain, M. N. Ahsan, R. Ali and M. U. M. Siddique, *ACS Omega*, 2021, **6**, 5033–5045.

38 International Council for Harmonisation (ICH), ICH harmonised guideline Q2(R2): Validation of analytical procedures, November 2023. Available at: [https://database.ich.org/sites/default/files/ICH\\_Q2R2\\_Guideline\\_2023\\_1116\\_1.pdf](https://database.ich.org/sites/default/files/ICH_Q2R2_Guideline_2023_1116_1.pdf) (accessed 2 July 2025).

39 International Council for Harmonisation (ICH), *ICH Harmonised Guideline: Q12 – Technical and Regulatory Considerations for Pharmaceutical Product Lifecycle Management*, 2019, available at: <https://www.ich.org/page/quality-guidelines> (accessed October 2025).

40 United States Pharmacopeia (USP), *General Chapter <1469> –Residual Solvents*, United States Pharmacopeia and National Formulary (USP–NF), United States Pharmacopeial Convention, Rockville, MD, 2023, available at: <https://www.uspnf.com> (accessed October 2025).

41 S. Nakka, N. K. Katari, S. K. Muchakayala, S. B. Jonnalagadda and S. Manabolu, *ACS Omega*, 2024, **9**, 8773–8788.

42 J. Peng, C. Ge, K. Shang, S. Liu and Y. Jiang, *Pharm. Biol.*, 2024, **62**, 480–498.

43 Y. Lou, Z. Sun, Y. Chai, H. Qin, Q. Hu, Y. Liu, X. Zheng, Y. Hu, M. Bao, J. Gu and Y. Zhang, *J. Chromatogr. B: Anal. Technol. Biomed. Life Sci.*, 2023, **1229**, 123871.

44 J. Y. Lu, Z. Q. Bu, Y. Q. Lei, D. Wang, B. He, J. Wang and W. T. Huang, *J. Mol. Liq.*, 2024, **409**, 125503.

45 K. Thakkar, R. Solanki and R. Patel, *Sep. Sci. Plus*, 2025, **8**, 8.

46 R. Patel, S. Purohit, R. Solanki, D. Khunt, C. Patel, R. Patel and S. Parikh, *Rapid Commun. Mass Spectrom.*, 2023, **37**, e9488.

47 R. Patel, M. Patel, R. Solanki and D. Khunt, *Ann. Pharm. Fr.*, 2024, **82**, 771–779.

48 I. N. Bhukya and D. P. Beda, *Green Anal. Chem.*, 2024, **8**, 100090.

49 F. Pena-Pereira, W. Wojnowski and M. Tobiszewski, *Anal. Chem.*, 2020, **92**, 10076–10082.

50 F. R. Mansour, J. Płotka-Wasylka and M. Locatelli, *Analytica*, 2024, **5**, 451–457.



51 N. Manousi, W. Wojnowski, J. Plotka-Wasylka and V. Samanidou, *Green Chem.*, 2023, **25**, 7598–7604.

52 P. M. Nowak, W. Wojnowski, N. Manousi, V. Samanidou and J. Plotka-Wasylka, *Green Chem.*, 2025, **27**, 5546–5553.

53 F. R. Mansour and P. M. Nowak, *BMC Chem.*, 2025, **19**, 121.

54 P. Prajapati, R. Dhameliya, R. Jha, P. Shah, V. S. Pulusu, A. Haque, S. Ahmad and S. Shah, *Chem. Afr.*, 2024, **7**, 3717–3730.

55 P. Prajapati, M. Patel, Y. Kansara, P. Shah, V. S. Pulusu and S. Shah, *Sustainable Chem. Pharm.*, 2024, **39**, 101523.

56 P. Prajapati, A. Shahi, A. Acharya, V. S. Pulusu and S. Shah, *J. Chromatogr. Sci.*, 2023, **11**, 938–952.

57 P. Prajapati, B. Rana, V. S. Pulusu and A. Mishra, *Chem. Afr.*, 2023, **7**, 1385–1400.

58 P. Prajapati, M. Salunkhe, V. S. Pulusu and S. Shah, *Chem. Afr.*, 2023, **7**, 1353–1371.

